Published in final edited form as:
Biochemistry. 2012 January 10; 51(1): 329–341. doi:10.1021/bi201380p.

CYCLOSTREPTIN DERIVATIVES SPECIFICALLY TARGET CELLULAR TUBULIN AND FURTHER MAP THE PACLITAXEL SITE†

Enrique Calvo[&,1], **Isabel Barasoain**[&,*,2], **Ruth Matesanz**[2], **Benet Pera**[2], **Emilio Camafeita**[1], **Oriol Pineda**[3], **Ernest Hamel**[4], **Christopher D. Vanderwal**[5], **José Manuel Andreu**[2], **Juan A. López**[1], and **José Fernando Díaz**[*,2]

[1]Unidad de Proteómica, Centro Nacional de Investigaciones Cardiovasculares, CNIC, Madrid, Spain.

[2]Centro de Investigaciones Biológicas, CIB, CSIC, Madrid, Spain.

[3]Facultat de Química, Universitat de Barcelona, Av. Diagonal 647, 08028, Barcelona, Spain.

[4]Screening Technologies Branch, Developmental Therapeutics Program, Division of Cancer Treatment and Diagnosis, National Cancer Institute at Frederick, National Institutes of Health, Frederick, Maryland 21702.

[5]Department of Chemistry, University of California at Irvine, Irvine, California 92697.

Abstract

Cyclostreptin is the first microtubule stabilizing agent whose mechanism of action was discovered to involve formation of a covalent bond with tubulin. Treatment of cells with cyclostreptin irreversibly stabilizes their microtubules because cyclostreptin forms a covalent bond to β-tubulin at either the T220 or the N228 residue, located, respectively, at the microtubule pore and luminal taxoid binding sites. Due to its unique mechanism of action, cyclostreptin overcomes P-glycoprotein-mediated multidrug resistance in tumor cells.

We used a series of reactive cyclostreptin analogues, 6-chloroacetyl-cyclostreptin, 8-chloroacetyl-cyclostreptin, and [^{14}C-acetyl]-8-acetyl-cyclostreptin, to characterize the cellular target of the compound and to map the binding site. The three analogues were cytotoxic and stabilized microtubules in both sensitive and multidrug resistant tumor cells. In both types of cells, we identified β-tubulin as the only or the predominantly labeled cellular protein, indicating that a covalent binding to microtubules is sufficient to prevent drug efflux mediated by P-glycoprotein.

6-chloroacetyl-cyclostreptin, 8-chloroacetyl-cyclostreptin, and 8-acetyl-cyclostreptin labeled both microtubules and unassembled tubulin at a single residue of the same tryptic peptide of β-tubulin as was labeled by cyclostreptin (219-LTTPTYGDLNHLVSATMSGVTTCLR-243), but labeling with the analogues occurred at different positions of the peptide. 8-Acetyl-cyclostreptin reacted either with T220 or N228, as did the natural product, while 8-chloroacetyl-cyclostreptin formed a cross link to C241. Finally 6-chloroacetyl-cyclostreptin reacted with any one of the three residues,

†This work was supported in part by grant BIO2010-16351, Ministerio de Ciencia e Innovación (to JFD). The CNIC is supported by the Ministerio de Ciencia e Innovación and the Fundación Pro CNIC.

*Corresponding Authors: Cell Biology: Dr. Isabel Barasoain, Biochemistry and modeling: Dr. J. Fernando Díaz, Centro de Investigaciones Biológicas, Consejo Superior de Investigaciones Científicas, C/ Ramiro de Maeztu, 9, 28040 Madrid, España, phone: +34-918373112 ext 4269, fax: +34-915360432, fer@cib.csic.es.
&These authors contributed equally to this work.

Supporting information about the MS analysis is available. This material is available free of charge via the internet at http://pubs.acs.org

thus labeling the pathway for cyclostreptin-like compounds, leading from the pore where these compounds enter the microtubule to the luminal binding pocket.

The increase in life expectancy and the decrease in mortality due to infectious diseases have turned cancer into one of the major causes of death in developed countries. Although neoplastic diseases usually start as localized disease, metastatic processes turn it into a systemic disease for which systemic treatment, such as the use of chemotherapeutic agents, is required. The search for new and more effective treatments is a field of the utmost importance in current drug discovery and clinical research (1).

Microtubule stabilizing agents[1] (MSAs) are one of the most successful classes of antitumor agents used in the clinical treatment of neoplastic diseases. The archetypes of this class are paclitaxel (PTX) (2) and docetaxel, with two newer approved agents being the taxoid cabazitaxel (3) and the epothilone ixabepilone (4). PTX preferentially binds to microtubules (MTs), the assembled form of tubulin, displacing the assembly equilibrium between dimeric and polymeric tubulin towards the latter. Since proper functioning of this assembly/disassembly equilibrium is essential for normal cell division, compounds that bind either form of tubulin target rapidly dividing cells, including tumor cells, arresting them in mitosis, and ultimately killing them through apoptosis.

The search for compounds with a similar mechanism of action as PTX but with improved chemical (such as, ease of synthesis) or pharmacological properties (such as, better bioavailability, lower toxicity, less prone to cause resistance) led to the discovery of a number of new chemotypes with essentially the same biological mechanism of action. Except for laulimalide and peloruside A (5–6), which both bind at a different site, most of these newer compounds [e. g., epothilones (7), discodermolide (8), and cyclostreptin (Cs) (9)] are PTX biochemical mimetics, since they interfere with PTX binding to MTs and induce tubulin assembly (10). Thus, the PTX site in tubulin is able to accommodate with high affinity many different chemical scaffolds. Moreover, the kinetic analysis of studies of interactions of fluorescent PTX derivatives with MTs led to the proposal of at least a second, intermediate site that accommodates taxoid site MSAs either transiently (11) or permanently (12) on their way to the MT lumen (13). Recent investigations by our group suggest that the interaction of MSAs with these secondary site(s) occurs in at least two different structural manners (14), (15).

Covalent labeling of proteins is a powerful tool that has been used extensively for identification of acceptor molecules in heterogeneous mixtures and in the selective labeling of receptor sites in biological systems. The labeling methods make use of the reactivity of one or more common functional groups on the surface of protein molecules. A common approach to obtain a specific label on a protein is the conjugation of a thiol-reactive group onto a ligand so that it will cross link to a solvent accessible cysteine residue close to the ligand binding site (16). Such cysteine residues can be specifically labeled with derivatives of haloacetyl compounds, with disulfide reactive compounds or with maleimide. After cross linking is successfully achieved, digestion and mass spectrometry experiments are used to determine which segment of the protein reacts with the ligand (17).

[1] **6CA-Cs**, 6-chloroacetyl-cyclostreptin, **8Ac-Cs**, 8-acetyl-cyclostreptin, **8CA-Cs**, 8-chloroacetyl-cyclostreptin, **[^{14}C]8Ac-Cs**, [^{14}C-acetyl]-8-acetyl-cyclostreptin, **Cs**, cyclostreptin, **DMSO**, Dimethyl sulfoxide, **GAB**, Glycerol Assembly Buffer (3.4 M glycerol, 6 mM $MgCl_2$, 1 mM EGTA, 10 mM sodium phosphate buffer, pH 6.7), **HRMS**, high resolution mass spectrometry, **MALDI**, matrix-assisted laser desorption/ionization, **MDR**, multidrug resistant and multidrug resistance, as appropriate, **MS**, mass spectrometry, **MS/MS**, tandem mass spectrometry, **MSA**, microtubule stabilizing agent, **MT**, microtubule, **NMR**, nuclear magnetic resonance, **PIS**, precursor ion scanning, **PTX**, paclitaxel, **P-gp**, P-glycoprotein, **PVDF**, polyvinylidene fluoride, **Q1**, quadrupole 1, **Q3**, quadrupole 3, **SDS**, sodium dodecyl sulfate, **SRM**, selected reaction monitoring.

Cs is a natural product from *Streptomyces* sp. 9885 (18–19) with a novel mechanism of action. This compound is the first MSA discovered that reacts covalently with tubulin. Cs treatment of cells irreversibly stabilizes their MTs by covalent binding to tubulin, exactly as occurs with purified tubulin, and causes cell cycle arrest. The compound reacts through the PTX sites on β-tubulin by cross linking to either Thr220 or Asn228 (in this paper, we use the residue numbering of Nogales et al., 1998), but not to both, on a single β-tubulin molecule. These observations provided invaluable information about the interaction of this MSA with both the pore and luminal sites involved in binding to the taxoid site (20).

Due to its unique mechanism of action, Cs (20) and related analogues, as we will show here, overcome P-glycoprotein- (P-gp) mediated multidrug resistance (MDR) in tumor cells. While many tumors initially respond favorably to chemotherapy, effective tumor response is frequently limited by the development of resistance. One of the main causes of resistance is MDR, caused by over-expression of several trans-membrane proteins with drug efflux activity, the most prominent example being P-gp (21), a member of the ATP binding cassette family with broad substrate specificity. The extent of drug resistance in human tumors correlates well with P-gp over-expression (22). The overall result of this over-expression is a reduction of the intracellular drug concentration. Although cells over-expressing P-gp are in fact sensitive to taxoids because they can still be killed by higher concentrations of these drugs, they reduce the effective concentration to which they are exposed. Moreover, non-tumor cells are effectively killed at those higher concentrations because of their inability to reduce the intracellular drug concentration, instead of being differentially spared because of their lower division rate. It would seem likely that a compound with a covalent mechanism of action, such as Cs, would have limited access to an efflux pump, making over-expression of P-gp irrelevant.

Since the previous results suggest that covalent binders targeting the paclitaxel sites might become a potential new approach for the design of clinically useful drugs, we employed Cs derivatives with three different reactive moieties, with the intention of improving our understanding of the cellular and biochemical mechanism of action of Cs by pursuing two different objectives. First, we wanted to evaluate the possible cytotoxicity of Cs based on additional targets. In order to do this, we employed 8-acetylcyclostreptin (8Ac-Cs) (Figure 1), a compound with the same reactive moiety as Cs, into which we incorporated a radiolabel. The compound has been previously used as a bona-fide probe of Cs binding to MTs (23) and is used in this work to label tumor cells with the intention of detecting possible cross links with other cellular proteins.

Second, we wanted to explore the possibility that there were additional reactive residues in the paclitaxel binding sites. To do this, a thiol-reactive chloroacetyl group was introduced at either position 6 or position 8 of Cs (Figure 1), thereby potentially converting the molecule into a bifunctional reactive agent to permit further characterization of the interaction of Cs with the luminal and pore binding sites.

The results presented in this work indicate that Cs and the analogues all are active against sensitive and P-gp over-expressing cells. The use of the radiolabeled probe indicated that Cs labeling of cellular tubulin is specific and that no major competing reaction occurred in any of the tumor cell lines examined. The modified compounds retained their activity, being able to covalently react with tubulin at the previously described sites and, in addition, at Cys241, allowing more detailed mapping of the ligand into the pore and luminal sites.

EXPERIMENTAL PROCEDURES

Preparation of tubulin and MTs

Electrophoretically homogeneous bovine brain tubulin and synthetic Cs were prepared as described (24–25), tubulin from 1A9 cells was prepared as described, using A549 cells (20). Mildly cross linked, stabilized MTs were prepared as described previously (11, 26), and the concentration of taxoid sites in the preparation was determined as described (26).

Synthesis of Cs derivatives

The synthesis and characterization data for 8Ac-Cs and [^{14}C]8Ac-Cs (20 mCi/mmol) were published previously (23). The synthesis of 8CA-Cs was performed in a completely analogous manner, substituting acetyl chloride with chloroacetyl chloride; the minor product of this reaction was 6CA-Cs. The identities of the compounds were confirmed by 1D NMR and HRMS. 6CA-Cs *m/z* 477.2035 $(M + H)^+$ (calcd $C_{26}H_{34}ClO_6$ 477.2044) + 499.1855 $(M+Na)^+$ (calcd $C_{26}H_{33}ClO_6Na$ 499.1863). 8CA-Cs *m/z* 477.2033 $(M + H)^+$ (calcd $C_{26}H_{34}ClO_6$ 477.2044) + 499.1854 $(M+Na)^+$ (calcd $C_{26}H_{33}ClO_6Na$ 499.1863). 1H NMR 6CA-Cs (Cl_3CD 500 MHz) δ 5.42 (1H, s), 4.74 (1H, dd, *J*=4.5, 9.2), 4.39 (1H, brs), 4.16 (1H, d, *J*=14.6), 4.14 (1H, d, *J*=14.6) 3.80 (1H, brs), 3.22 (1H, d, *J*=9.0), 2.82 (1H, m), 2.60 (1H, t, *J*=9.0), 2.57 (1H, m), 2.35 (1H, dd, *J*=8.5, 13.7), 2.31-2.12 (3H, m), 2.06 (1H, m), 1.99 (1H, m), 1.85 (1H, m), 1.77 (3H, s), 1.71 (1H, s), 1.63 (1H, s), 1.43 (3H, s), 1.27 (5H, d + m, *J*=7.2 (d)), 1.11 (1H, d, *J*=7.0), 8CA-Cs (Cl_3CD 500 MHz) δ 5.31 (1H, s), 4.85 (1H, d, *J*=4.9), 4.47 (1H, brs), 4.06 (2H, s), 3.80 (1H, brs), 3.58 (1H, m), 3.44 (1H, d, *J*=9.3), 2.90 (1H, m), 2.61 (1H, m), 2.55 (1H, t, *J*=9.6), 2.36 (1H, dd, *J*=13.7, 7.7), 2.07 (2H, m), 1.97 (1H, m), 1.85-1.65 (6H, m), 1.65-1.53 (1H, m), 1.47 (3H, s), 1.40-1.28 (2H, m), 1.27 (3H, d, *J*=7.0), 1.13 (1H, d, *J*=7.5).

Cell biology

Human A549 non-small lung carcinoma and human ovarian carcinoma 1A9, A2780 and A2780AD (MDR over-expressing P-gp) cells were cultured as previously described (20). Indirect immunofluorescence and cell cycle analysis was performed as described (10). Cytotoxicity assays were performed with a modified MTT assay (27).

Two dimensional polyacrylamide gel electrophoresis and electroblotting

Proteins were extracted from cell pellets as described (28). Protein extracts (50 μg) were labeled with 400 pmol of the *N*-hydroxysuccinimide ester of Cy2 fluorescent cyanine dye on ice in the dark for 30 min according to the instructions of the manufacturer (GE Healthcare). The labeling reaction was quenched with 1 μL of 10 mM lysine on ice for 10 min in the dark, and protein extracts were diluted in Rehydration Buffer (7 M urea, 2 M thiourea, 2% 3-((3-cholamidopropyl)dimethylammonio)-1-propanesulfonic acid), reduced with 50 mM dithiolthreitol, and applied by cup-loading to 18 cm immobilized pH gradient strips pH 3-11NL (GE Healthcare), which was previously rehydrated with Rehydration Buffer containing 100 mM hydroxyethyl disulfide (DeStreak, GE Healthcare), as described (29). Then the proteins were separated on 10% Tris–glycine PAGE-SDS gels at 25 °C until the tracking dye had migrated off the bottom of the gel. Later, gels were scanned with a Typhoon 9400 scanner (GE Healthcare) at 100 μm resolution using appropriate wavelength and filter for the Cy2 dye.

After imaging, proteins on the gel were transferred onto polyvinylidene fluoride (PVDF) membranes (Immobilon-P, Millipore) by semi-dry electroblotting using Tris/Glycine Transfer Buffer (Biorad) containing 10% methanol. The transfer conditions were 0.8 mA/cm^2 for 1 h at room temperature in a Hoefer TE77 semi-dry transfer unit (GE Healthcare). After transfer, PVDF membranes were scanned with the Typhoon 9400 scanner for Cy2 dye

location. The [^{14}C]-labeled proteins were detected by exposing the membranes to a BAS-MS 2340 imaging plate (5 days), which was scanned with a Fuji 3000 phosphorimager. The images were used for cutting out the labeled spots for further analysis by matrix-assisted laser desorption/ionization (MALDI) mass spectrometry (MS).

In-gel protein digestion and identification of proteins by MALDI MS

Protein spots were excised from replicated gels and transferred to pierced V-bottom 96-well polypropylene microplates (Bruker Daltonik, Bremen, Germany) loaded with ultrapure water. The samples were digested automatically using a Proteineer DP robot (Bruker Daltonik) according to the protocol of Shevchenko et al. (30).

MALDI analyses were performed in an Ultraflex MALDI-TOF/TOF mass spectrometer (Bruker Daltonik) as described by (31). MALDI-MS and Tandem Mass Spectrometry (MS/MS) data were combined through the BioTools 3.0 program (Bruker Daltonik) to search a non-redundant protein database (NCBInr 20090809, ca. 7•10^6 entries, National Center for Biotechnology Information, Bethesda, MD, USA) using the Mascot 2.2.1 software (Matrix Science, London, UK) (31).

Binding of Cs derivatives to MTs

Samples containing cross linked MTs (25 μM taxoid sites) and 20 μM Cs derivatives were incubated for 60 min at 37 °C in a solution containing 3.4 M glycerol, 10 mM NaPi, 1 mM EGTA and 6 mM $MgCl_2$, pH 6.7 (GAB) plus 0.1 mM GTP. MTs were pelleted by centrifugation in a TLA 100 rotor at 90000 × g for 20 min. Samples were processed and extracted as described (20), with each organic extract residue dissolved in 60 μL of methanol. Ligands reversibly bound to pelleted polymer and ligands in the supernatant were detected by HPLC analysis (20).

The kinetics of the binding of the compounds to stabilized cross linked MTs was estimated by incubating 50 nM Flutax-2 and cross linked MTs (50 μM taxoid sites) with increasing amounts of the compound for 30 min at 35 °C. The amount of Flutax-2 still bound to the MTs was measured and the data analyzed as described (9–10). However, given the covalent nature of the Cs-MT interaction, the apparent binding constant determined as described in (26) would be the concentration of the compound required to displace 50% of the Flutax-2 bound in 30 min, and this provides an estimate of the kinetics of the reaction.

Sample preparation and in-solution protein digestion for MS analyses

Samples of labeled cross linked MTs were prepared by incubating them (concentration, 20 μM taxoid sites) with 25 μM Cs derivatives for 30 min at 25 °C in GAB plus 0.1 mM GTP. Alternatively, samples containing cross linked MTs (10 μM taxoid sites) and 20 μM Cs were preincubated for 30 min at 25 °C in GAB plus 0.1 mM GTP. Then 35 μM 8CA-Cs or 6CA-Cs was added, and the sample was incubated another 60 min at 37 °C to estimate the nonspecific reactivity of 8CA-Cs or 6CA-Cs. The sample was processed and analyzed as described above. MTs were collected by centrifugation in a TLA 100 rotor at 90000 × g for 20 min. Pellets were washed twice with water and suspended in 200 μL of 50 mM NH_4HCO_3, 12 mM EDTA and 0.01% SDS, pH 7.6. Unassembled tubulin samples were prepared using 20 μM GTP-tubulin in 10 mM NaPi, 1 mM EDTA, 0.1 mM GTP, pH 7.0 without (for dimeric tubulin) or with (for oligomeric tubulin) 1.5 mM $MgCl_2$ and 2.5% dimethyl sulfoxide (DMSO) or 25 μM drug. Samples were centrifuged as described above to remove aggregates, and 20 μL was diluted 1:1 into 50 mM NH_4HCO_3 and digested with trypsin (1 μg sequencing grade, Promega, 2 h, 37 °C). Reaction mixtures were dried *in vacuo* and, for analysis, the residue was dissolved in 5% CH_3CN, 0.5% CH_3COOH.

Off line nanospray analysis for Cs derivatives molecule characterization

About 1 μL of Cs derivative solutions in DMSO containing 10 μg of the ligand was dissolved in 20 μL of 50% CH_3CN, 0.5% CH_3COOH in water. 5 μL of the preparation was introduced in the off line nanospray needle (medium needle, Protana, Odense, Denmark) and analyzed in a hybrid triple-quadrupole mass spectrometer (4000 Q-Trap LC/MS-MS system, Applied Biosystems/MDS Sciex, Concord, ON, Canada) according to the protocol detailed in (20).

Nano-liquid chromatography and MS analysis of tryptic peptides

To identify the residues labeled by Cs and derivatives, the resulting tubulin-derived tryptic peptides from control and samples treated with a Cs derivative were subjected to liquid chromatography coupled to tandem MS in the 4000 Q-trap system (Applied Biosystems/MDS Sciex) as described in (20). Combined analyses were designed to perform the corresponding precursor ion scanning (PIS) and selected reaction monitoring (SRM) experiments as described in supplemental information. For peptide identification, all MS and MS/MS spectra were analyzed with Analyst 1.5 software (Applied Biosystems).

For high resolution analyses, tryptic peptide mixtures were also injected onto a C-18 reversed phase nano-column (100 μm I.D. × 12 cm, Mediterranea sea, Teknokroma) and analyzed in a continuous CH_3CN gradient consisting of 0–40% B in 90 min, 50–90% B in 1 min (B=95% CH_3CN, 0.5% CH_3COOH in water). A flow rate of 300 nL/min was used to elute peptides from the reverse phase nano-column to an emitter nanospray needle for real time ionization and peptide fragmentation on an orbital ion trap mass spectrometer (LTQ-Orbitrap XL, Thermo-Fisher). An enhanced resolution spectrum (resolution=60000) followed by the MS/MS spectra from the five most intense parent ions were analyzed during the chromatographic run (130 min). Dynamic exclusion was set at 0.5 min. For peptide identification, all spectra were analyzed with Xcallibur 2.7.0 software (Thermo Fisher).

Molecular modeling

Models of the modified Cs analogues bound in the PTX pore site were constructed as described in (20). In short, the modified analogues were built over the model of Cs bound to the pore site reported previously (20), and MacroModel was used to find the final conformations of each analogue (MonteCarlo conformational search, 10000 iterations, AMBER* force field, H_2O/GBSA). To account for the reaction of the analogues with Cys241 in the extended luminal site, the conformation of the B9–B10 loop of β-tubulin was relaxed as reported in (32). Then, the chloroacetyl analogues were built over this extended model of the taxoid site, and MacroModel was used again to find their final conformations. Finally, the binding of the analogues to Asn228 was rationalized as follows: docking simulations of each analogue were performed with AutoDock over the most suitable structures of tubulin (1TUB, 1JFF and 1TVK entries of the PDB), as reported in (32), searching for their preliminary non-covalent interactions with the luminal site. In their best scored complexes, the reactive strained lactone was placed near the region of Asn228, which could therefore attack it.

The transition state for the reaction of the chloroacetyl derivatives with the Cys β-241 was modeled using Spartan '08, version 1.1.2, Build 131 at the B3LYP 6-31G* level of theory in ethanol (implicit ethanol) (33–34) (See Supplemental Information for details).

RESULTS

Cytotoxic Cs derivatives overcome resistance in MDR cells and arrest the cell cycle in G2/M phase

In our previous work (20), we showed that Cs is a bona fide mitotic inhibitor with a PTX-like cellular mechanism. However, it reacts covalently with tubulin, and its effects become irreversible. In order to determine if the modifications introduced at Cs positions 6 and 8 did not significantly alter the biological properties of the compound, the cytotoxicity of these ligands as compared with Cs was determined in 1A9 and A2780AD ovarian carcinoma cells. The compounds studied were cytotoxic to both sensitive and MDR cells. Their IC50 values were higher than that of the parental compound (Table I), indicating that positions 6 and 8 are important in MT binding. The [^{14}C]labeled and nonradiolabeled 8-acetyl compounds had similar cytotoxicity. All compounds had similar IC50 values for cells over-expressing P-gp (A2780AD) and their isogenic sensitive pair (1A9), suggesting that all of them retain the covalent mechanism of action and that this mechanism of action is able to overcome P-gp mediated MDR.

We next determined the effect of a 24 h incubation with serial concentrations of these ligands on the MT network of A549 cells (Figure 2, upper panel). Similar MT bundles in interphase cells were induced with 500 nM Cs, 2.5 μM 8Ac-Cs, 2.5 μM [^{14}C]8Ac-Cs, 2.5 μM 6CA-Cs or 5 μM 8CA-Cs. We then determined the ligand concentrations that induced maximal arrest in the G2/M phase of the cell cycle of 1A9, A2780AD and A549 cells (Figure 2, lower panel). Maximal arrest was obtained with 100 nM Cs, 400 nM 8Ac-Cs, 400 nM [^{14}C]8Ac-Cs, 200 nM 6CA-Cs or 400 nM 8CA-Cs.

Tubulin is the main Cs-reacting protein in cells

We purified tubulin from 1A9 cells treated with 50 nM Cs, close to the IC50, and determined that under these conditions only ~15% of the cellular β-tubulin had reacted with Cs. However, the important question remained of whether any other cellular proteins might be reacting with Cs or whether this compound more specifically reacts with tubulin. In order to determine which are the cellular proteins targeted by Cs, we employed [^{14}C]8Ac-Cs. To find such proteins, we treated A549, 1A9 and A2780AD with either a low (300 nM, inducing mitotic arrest) or a high concentration of the compound (2.5 μM, inducing many cytoplasmic MT bundles) for 24 h. Cells were recovered from the flasks and washed exhaustively with phosphate-buffered saline. We then extracted treated cells and subjected the proteins to two-dimensional polyacrylamide gel electrophoresis. The separated proteins were electroblotted for detection of radiolabeled species (Figure 3 A,B). In the case of A549 cells incubated with 2.5 μM [^{14}C]8Ac-Cs, an intense band (>99%) and three faint spots were obtained. The intense signal (spot 1 Figure 3 A,B) was identified as β-tubulin by MALDI-TOF MS analysis, while the three minor spots were identified as an elongation factor 1-δ (spot 2), aldehyde dehydrogenase (spot 3) and T-complex protein 1 subunit (spot 4). These results indicated that [^{14}C]8Ac-Cs interacts mainly with cellular β-tubulin and implied that this is likely for Cs and the other derivatives, too. We extended these results to other cell lines (1A9 and A2780AD) and drug concentrations, obtaining in most cases a scanned image of only one radiolabeled spot corresponding to β-tubulin (Figure 3, C,D,E). The results obtained with the A2780AD line (not shown) were similar to those obtained with the sensitive line.

Binding to MTs and displacement of Flutax-2

In order to confirm that the compounds retained the same mechanism of action as Cs, the covalent binding of the compounds to cross linked, stabilized MTs was confirmed using an HPLC assay (Figure 3 F,G). The compound was incubated in the presence and in the

absence of MTs, the solution centrifuged and the supernatant and MT pellet extracted and analyzed. 6CA-Cs was found stable in solution in the absence of MTs (Figure 3F). However, in the presence of MTs the compound disappeared from the supernatant, and it was not possible to extract it from the MT pellet (Figure 3G), as would be expected for a compound that binds irreversibly to MTs (20) (all other compounds behaved identically, not shown).

The compounds were tested for their ability to displace Flutax-2, a bona fide fluorescent PTX biomimetic, from stabilized, cross linked MTs (10). All three compounds tested were found to displace Flutax-2 from its binding site with different apparent affinities (Kd_{app}35 °C Cs=49±3 nM (9), 8Ac-Cs=555±100 nM, 6CA-Cs=141±16 nM, 8CA-Cs=400±43 nM). Given the fact that a covalent reaction is observed, the displacement assay does not measure a true dissociation constant, as is the case for compounds that do not bind covalently (10, 35). Instead, what is measured is the concentration of compound necessary to displace 50% of the bound Flutax-2 in 30 min. Since the reaction observed is bimolecular, the kinetic rate would depend linearly on the concentration of the reactants. Thus, the difference in the concentration required to bind to the same amount of tubulin in 30 min (thus displacing the same amount of Flutax-2) reflects the different kinetic rates of the reaction with the different compounds, with the smallest value being the one for the most active, fastest binding compound.

As was the case for cytotoxicity, Cs was the most active of the compounds, with an apparent dissociation constant at 35 °C 3 times smaller than that of 6CA-Cs, 8 times smaller than that of 8CA-Cs and 11 times smaller than that of 8Ac-Cs, indicating a moderate influence of the substituents on the kinetics of the covalent reaction.

Interaction of the Cs derivatives with assembled MTs

Having established that the three derivatives, like Cs, reacted covalently with β-tubulin, we confirmed the covalent binding of the Cs derivatives to MTs by incubating them with preformed, stabilized, cross linked MTs in GAB. The samples treated with Cs derivatives, together with the untreated control, were digested with trypsin, and the corresponding tryptic peptide mixtures were analyzed by MALDI-TOF MS. We identified the adducts for the different Cs derivatives, demonstrating that all the modified compounds were active, and covalently reacted with β-tubulin in MTs (Figure S1).

To identify the reactive amino acid residues with each derivative, we performed PIS analyses for the filtering of peptide ions joined to each Cs derivative. Firstly, the fragmentation spectra of 6CA-Cs, 8CA-Cs and 8Ac-Cs were determined by enhanced resolution analysis in a triple-quadrupole mass spectrometer for the identification of fragment ions that provides better signal (diagnostic ion) for the ion filtering experiments. For that, the exact mass of each Cs derivative was determined (Figures S2A and S2B), and then these exact masses were selected for fragmentation by collision-induced dissociation (CID) (Figures S2C and S2D). The fragment masses obtained from these experiments were checked as potential diagnostic ions for later ion filtering experiments by PIS analyses, in which the diagnostic ion allows the detection of the parent molecule. The examination of PIS experiments using different fragment ions with 8Ac-Cs (Figure S3A) and 6 or 8CA-Cs (Figure S3B) led to the selection of the fragment ion at 249 *m/z* as the diagnostic ion for ion filtering experiments. This ion appeared with high intensity in the fragmentation spectra from all Cs derivatives (Figures S2C and D).

Then we confirmed the covalent binding of the Cs derivatives to microtubules by incubating them with preformed, stabilized, cross linked MTs in GAB. The samples treated with Cs derivatives, together with the untreated control, were digested with trypsin, and the corresponding tryptic peptide mixtures were analyzed by MALDI-TOF MS. We identified

the adducts for the different Cs derivatives, demonstrating that all the modified compounds were active and covalently reacted with β-tubulin in MTs (Figure S1).

The exact residue labeled was determined by PIS analysis of the tryptic peptide mixtures in a hybrid triple-quadrupole mass analyzer. The tubulin-derived tryptic peptide spanning β-residues 219–243 was found to be the labeled peptide for all the Cs derivatives, as had also occurred with Cs itself (20). However, the labeled residues varied, depending on the derivative used. The corresponding PIS chromatograms are displayed in Figure 4. When the MTs were incubated with 8Ac-Cs, two adducts were detected (ions 2 and 1 in Figure 4B). These adducts corresponded, respectively, to the 8Ac-Cs-linked tubulin peptide, and the same sequence bound to Cs, suggesting that 8Ac-Cs was not entirely stable. As expected, 8Ac-Cs reacted with tubulin at the same residues as the parent compound, Thr220 and Asn228 (20), thus indicating that the 8Ac-Cs labels MTs essentially as does Cs itself.

In contrast, when MTs were incubated with 6CA-Cs, a new adduct was detected (Figure 4C). As with 8Ac-Cs, the adducts corresponding to 6CA-Cs and Cs bound to tubulin at the Thr220 and Asn228 residues were detected (ions 2* and 1 in Figure 4C, respectively). In addition, a third adduct, in which the chloroacetylated derivative was linked to Cys241 through the acetyl group was unambiguously detected (ion 3 in Figure 4C). This demonstrated that the new reactive group at C-8 was able to label a Cys residue in the neighborhood of the PTX luminal binding site. Despite the fact that this new ion had the same mass as ion 2* when analyzed at low resolution, as in the triple-quadrupole mass spectrometer, both ions clearly differed in their retention times, since ion 3 elutes about three min earlier in the chromatogram. Moreover, ions 2* and 3 differ notably in their fragmentation patterns: the spectrum from the Cys241-linked peptide showed different y-series fragments, with the additional mass of the Cs derivative from y3 (Figure 4E and Figure S5). In addition, ions 2* and 3 differ by 1 Da when measured at high resolution (Figure S4).

The chloroacetylated compounds also were unstable during sample work-up, since the neutral loss of the chloroacetyl group was detected when these derivatives were bound to tubulin (ions 1 and 4 in Figure 4C). These two ions eluted at the same retention time, while the corresponding neutral loss signals differ by 4 Da (around 1.3 Da in a triply charged species) (Figure S4).

When the MTs were incubated with 8CA-Cs, the results were somewhat different, since the dominant signal was derived from the Cys241 linked adduct (ion 3 in Figure 4D). The reduced fraction of Cs linked to Thr220 or Asn228 was probably largely derived from Cs, which arose from partial dechloroacetylation of the 8CA-Cs.

A schematic representation for the structure of the four detected ions is shown in Figure 4F, and the high resolution exact masses are displayed in Figure S4.

In order to confirm the specificity of the reaction of the chloroacetylated compounds with Cys241, 10 μM sites in stabilized MTs were preincubated with 20 μM Cs for 30 min at 25 °C. After the preincubation, an excess (35 μM) of 6CA-Cs or 8CA-Cs was added. The sample was incubated an additional 60 min at 37 °C and subsequently analyzed by MS. When MTs were treated with excess Cs prior to addition of either chloroacetylated derivative, only the ion 4 signal, indicating reaction of Cs with β-tubulin, was clearly detected, and no Cys241 adduct was found (Figure S6). This result is in accord with the lack of nonspecific reactivity of the chloroacetyl moiety with amino acid residues near the PTX site. Earlier experiments with both 7-chloroacetylpaclitaxel and 10-chloroacetylpaclitaxel are in agreement with these findings with the Cs derivatives. Both PTX analogues induced tubulin assembly, leading to the synthesis of radiolabeled versions of both compounds

([^{14}C] labels in the chloroacetyl moieties). However, neither compound caused significant alkylation of native MTs, unless tubulin denaturation had occurred (E. Hamel, unpublished observations). These findings together indicate that the reactivity of the chloroacetylated Cs derivatives with Cys241 is specific and that in the binding process the reactive moieties must closely approach the cysteine residue (the chloroacetyl moiety is approximately 8 Å in length), in contrast to what was observed with the chloroacetylated PTX analogues.

Estimation of adduct abundance by SRM

Although PIS is a powerful MS technique allowing filtering and identification of the tubulin binding sites for each Cs derivative, it is not well suited to relative quantification of different species carrying the diagnostic ion (36). To determine the relative abundance of the corresponding tubulin-bound species (Thr220, Asn228 and Cys241), the tryptic digests were analyzed as described in the supplemental information using SRM, a doubly stage filtering methodology designed for targeted quantitative proteomics (36–37).

We were able to detect the four masses selected (ions 1 to 4) in the different samples (Figure 5). In the case of the 8Ac-Cs-treated MT samples, we detected ions 1 and 2. The acetylated adduct (ion 2 in Figure 5B) showed the highest intensity (66%) as compared with the Cs adduct (ion 1) (33%) (Figure 4B). The Cys241-bound adduct accounted for about a fourth (24%), while the Thr220 and Asn228 adducts of 6CA-Cs account together for the 44% of the total integrated intensity from the 6CA-Cs-treated sample (Figure 5C). The Cys241-bound adduct was virtually the only species detected in the 8CA-Cs-treated sample (Figure 5D) by SRM analysis.

Interaction of the Cs derivatives with unassembled tubulin

Since Cs was able to react with the pore PTX site (Thr220) in unassembled tubulin, the Cs derivatives were also tested with dimeric and oligomeric tubulin by SRM, because it is a high selective and sensitive mass spectrometric quantitative approach. We performed directed MS analyses, including the masses corresponding to ions 1, 2 and 3 (Figure 4) and the mass corresponding to the unmodified tubulin-derived tryptic peptide (labeled as Ctrl, Figure 5, lower panel). No significant differences were observed between the dimeric and oligomeric tubulin preparations (Figure 5 and Figure S7).

8Ac-Cs was the most reactive compound, yielding two detectable adducts corresponding to the acetylated and deacetylated signals of the compound following reaction with Thr220. In contrast, only the Cys241-linked adduct was detected when unassembled tubulin was treated with 8CA-Cs. This suggests that the presence of the chloroacetyl moiety prevented binding at the external pore site. On the other hand, three adducts (those labeled at Thr220 with and without the haloacetyl group and the Cys241-linked ion) were detected after 6CA-Cs treatment of dimeric tubulin samples (Figure 5, lower panel).

Model of Cs interaction with the pore and the luminal sites

The interaction of Cs with the pore site was modeled in our previous work (supplemental Figure 4 in (20)). The newly synthesized Cs derivatives were modeled in the same position (Figure 6A). Both 6-CA-Cs and 8Ac-Cs perfectly fit in the same binding pose, but this is not the case for the 8CA-Cs derivative. If 8CA-Cs is docked in the same binding pose (Figure 6B) (which would be required for the covalent reaction with Thr220), the chlormethyl group of the haloacetyl moiety at C-8 would have a severe steric clash with the side chain of Arg278 (red sphere in Figure 6B). However, in the case of 8Ac-Cs, the acetyl group is small enough not to collide with Arg278, thus allowing the reaction of the strained olefin with Thr220.

On the other hand, a covalent reaction of 6CA-Cs and 8Ac-Cs also occurred with Asn228. Although the polypeptide backbone containing Asn228 faces the luminal PTX site in our model (Figure 7A), the side chain of Asn228 points toward the exchangeable nucleotide site and is strongly involved in interactions with the nucleotide (38). As indicated in the Experimental Procedures, modeling of the compounds in the canonical PTX site indicates two areas where low energy binding poses could occur (Figures 7B and 7C). The first (Figure 7B) places the compounds with the reactive strained olefin of Cs, 8AcCs and 6CA-Cs close enough to Asn228 to rationalize the reaction if the side chain had enough conformational freedom to switch between the exchangeable nucleotide site and the PTX site. However, the model indicates that a bulky substituent at position C-8 would severely preclude this favorable binding pose, explaining the lack of a reaction of 8CA-Cs with Asn228.

The second binding pose (Figure 7D) places the ligands with the chloroacetyl groups close enough to the B9–B10 loop to attack Cys241. However, in the tubulin structures obtained either by X-ray crystallography (1FFX and 1SA0) (39–40) or by electron diffraction (1TUB and 1JFF) (38, 41) Cys241 is close to, but not directly accessible, to the PTX luminal binding pocket, being separated from it by the B9–B10 loop. The analogous loop in α-tubulin fills the corresponding cavity and is flexible enough to suggest that alternative conformations of the β-tubulin B9–B10 loop could provide access of ligands to the β-tubulin PTX binding cavity (Figure 7A). To model the interactions of the chloroacetylated analogues with Cys241, the B9–B10 loop was allowed to relax until the cavity was extended enough to expose the cysteine residue. In this extended luminal site, 6CA-Cs and 8CA-Cs could form a stable covalent complex with Cys241 (Figures 7D and 7E). These two covalent complexes were furthermore stabilized by hydrophobic interactions in the region of Phe272 and by polar interactions of both lactone carbonyls of the Cs compounds with Arg322. In addition, 6CA-Cs showed a hydrogen bond between the OH at position C-8 and Glu29. Similarly, 8CA-Cs showed a hydrogen bond between the OH at position C-6 and Ser238. These two interactions could be strong enough to account as well for the transient binding of unmodified Cs to the extended luminal site prior to its reaction with Asn228.

Given the high reactivity observed for Cys241 with chloroacetylated ligands, (42–44) we wanted to estimate the proximity of the sulfur atom of Cys241 to the chlorine-bearing carbon atoms of 6CA-Cs and 8CA-Cs for the occurrence of the observed covalent reactions. We therefore performed a simple transition state modeling experiment using methanethiol and methyl chloroacetate (see Experimental Procedures for details). The C–S bond distance taken from the transition state geometry was found to be 2.393 Å. The models presented in Figures 7D and 7E allowed for the approach of the chlorine-bearing carbon atoms of both chloroacetyl groups to within 3 Å of the Cys241 sulfur atom.

DISCUSSION

Previously (20), we described that covalent binding of a MSA to MTs is able to overcome the P-gp-mediated MDR resistance phenotype in several resistant cell lines, including A2780AD. Moreover, we found a similar result by using high affinity taxoids (35). The confirmation of the these results with a set of Cs derivatives suggests that the basis for overcoming resistance in these cases was a decrease in unbound, or free, intracellular drug to values significantly lower than the dissociation constant of the ligand for the membrane pump. These results indicate that P-gp-mediated MDR can arise primarily from enhancing efflux of the ligand, thus lowering its intracellular concentration, rather than interfering with the rate of ligand influx into the cell.

Cs specifically binds to tubulin in treated tumor cells

Cs is a natural compound containing two electrophilic reactive groups, a strained olefin and a lactone carbonyl. Several compounds with covalent mechanisms of action, interacting either with proteins (45–46) or with DNA (47–48) are currently used in clinical medicine. However, other compounds with the same type of mechanism have failed to find a clinical use, perhaps because of nonspecific reactivity with non-target proteins that could cause drug toxicity (49–50).

In order to evaluate the possibility of designing other MSAs that have a covalent mechanism of action, we examined the specificity of the Cs-tubulin interaction in cells treated with a radioactive analogue of Cs, [^{14}C]8Ac-Cs. This analogue has the same reactive moiety and mechanism of action (23). In cells, as had been the case with purified tubulin (23), [^{14}C]8Ac-Cs behaved in a manner indistinguishable from that of the natural product. Over 99% of the radiolabel was specifically incorporated into β-tubulin (Figure 3), with the remaining label incorporated into three other proteins when the cells were treated with a concentration of [^{14}C]8Ac-Cs 100 times greater than the IC50 of the compound.

Mapping Cs binding at the MT pore and luminal sites

We used Cs derivatives modified at the secondary alcohols at positions C-6 and C-8 to further study the interaction of Cs with the pore and luminal sites. Two new analogues in which a cysteine reactive haloacetyl moiety was linked to the oxygen atoms at positions C-6 and C-8 were synthesized, and the reactivity of 6CA-Cs and 8CA-Cs with the cysteine residues close to the taxoid sites allowed us to explore potentially the pathway from the pore site to the luminal site and the binding poses of the ligand in the luminal site.

Unlike what was found with docetaxel and discodermolide, (15) the pore binding site modeled for Cs in Buey et al (20) at the β-subunit does not require residues from other tubulin heterodimers. In agreement, the compounds bind both to the pore site in microtubules and in unpolymerized tubulin. However, this was not the case for the interaction of these compounds with the luminal site. While like Cs (20), 8Ac-Cs and 6CA-Cs react with Asn228 in MTs, they are not able to react with this residue in unpolymerized tubulin, indicating that, as expected from the large difference in affinities of docetaxel and discodermolide for the luminal site in dimeric and polymeric tubulin (15), there might be a structural difference in the luminal site between the assembled and the unassembled states as has been previously proposed (51–53). In contrast, both haloacetylated compounds reacted similarly with Cys241 in MT's and unassembled tubulin. This suggests that the accessibility of the reactive thiol should be similar in both tubulin species.

MS analysis of the adducts formed between the Cs derivatives and β-tubulin indicated an influence of the alcohol at C-8 in the tubulin-Cs interaction. Although the compound acetylated at position C-8 behaved essentially as did the lead compound in labeling Thr220 or Asn228 in MTs and Thr220 in unassembled tubulin, its haloacetylated equivalent failed to label either Thr220 or Asn228. This failure was observed in both MTs and unassembled tubulin. This indicates that the presence of a large group at position C-8 substantially perturbs the interaction of Cs with both the pore and luminal sites so that the nucleophilic attack on the strained olefin between positions C-2 and C-17 cannot occur.

On the other hand, both chloroacetyl analogues specifically labeled Cys241, one of the two cysteine residues in the vicinity of the luminal site. This residue is actually close to the colchicine site (40), and, although it is close to the PTX binding pocket, it is shielded from it by the B9–B10 loop in several well-described tubulin structures (1TUB, 1JFF, 1TVK). Cys241 is a known reactive residue in tubulin (42), which also reacts with MT destabilizing agents, such as modified colchicines (54) and halogenated sulfonamides (43–44), which also

inhibit colchicine binding to tubulin. Thus, it can be speculated that Cs derivatives could also reach this residue through the colchicine binding pocket. Although a nonspecific reaction cannot be fully discarded, given the high reactivity of Cys241, the blocking of the PTX site with Cs abolished the reactions of 6CA-Cs and 8CA-Cs with Cys241. This strongly points towards 6CA-Cs and 8CA-Cs binding to Cys241 through the PTX site, aided by the flexibility of the B9–B10 loop. Note that given the irreversible nature of the alkylation of Cys241 by 6CA-Cs and 8CA-Cs, the reaction would occur even if only a very small fraction of the B9–B10 loop were in the open state, and such a small fraction could not be observed in the 3D structures (13, 38).

Additional evidence that these analogues attack Cys241 from the PTX site is the observation that C-7 and C-10 chloroacetylated PTX derivatives did not react with Cys241 and our transition state modeling calculations, which indicated that a 3 Å distance between the chloroacetyl group and thiol is required for the reaction to occur. Thus, the most reasonable explanation for our findings that 6CA-Cs and 8CA-Cs react with Cys241 is that the B9–B10 loop is more flexible than might have been anticipated and that at least a small fraction of the loop is in an open conformation resulting in a PTX luminal site larger than previously believed. This hypothesis is, moreover, concordant with the substantial chemical promiscuity of the PTX site, where many different chemotypes bind with identical biochemical effects (10).

Regarding the adducts with Asn228, this residue is located in a potential path for the drugs from the pore site to Cys241. However, Asn228 is rather distant (18 Å) from Cys241, explaining the failure to detect adducts with 6CA-Cs and 8CA-Cs at both Asn228 and Cys241. Moreover, Asn228 is also essential for the binding of GTP/GDP at the exchangeable nucleotide site of tubulin. In fact, the interaction of Asn228 with the exchangeable site nucleotide should limit the ability of Cs to attack the side chain in the 1TUB, 1JFF, and 1TVK models. It therefore seems likely that the Asn228 side chain must have enough conformational freedom to oscillate between the exchangeable nucleotide site and the PTX site.

The set of amino acids mapped by Cs and its analogues show a path that PTX mimetic drugs might follow from the outside of the MT, through the type I pore (Thr220), to reach the luminal site indicated by the 1TUB, 1JFF, and 1TVK models (Asn228), and to arrive finally at the extended luminal site (Cys241). One can readily imagine PTX mimetic agents of diverse chemical structures finding different areas of the extended luminal site where they have maximal affinity.

Supplementary Material

Refer to Web version on PubMed Central for supplementary material.

Acknowledgments

We thank Dr. Dmitriy Uchenik (UC Irvine) for performing the transition state model calculations, Prof. Javier Cañada for the help with the interpretation of the NMR spectra, Rhône Poulenc Rorer Aventis for supplying the docetaxel and Matadero Municipal Vicente de Lucas de Segovia for providing the calf brains for tubulin purification.

REFERENCES

1. Jemal A, Thomas A, Murray T, Thun M. Cancer statistics, 2002. CA Cancer J Clin. 2002; 52:23–47. [PubMed: 11814064]

2. Schiff PB, Fant J, Horwitz SB. Promotion of microtubule assembly in vitro by taxol. Nature. 1979; 277:665–667. [PubMed: 423966]
3. Galsky MD, Dritselis A, Kirkpatrick P, Oh WK. Cabazitaxel. Nat Rev Drug Discov. 2010; 9:677–678. [PubMed: 20811375]
4. Dumontet C, Jordan MA, Lee FF. Ixabepilone: targeting βIII-tubulin expression in taxane-resistant malignancies. Mol Cancer Ther. 2009; 8:17–25. [PubMed: 19139109]
5. Pryor DE, O'Brate A, Bilcer G, Díaz JF, Wang Y, Kabaki M, Jung MK, Andreu JM, Ghosh AK, Giannakakou P, Hamel E. The microtubule stabilizing agent laulimalide does not bind in the taxoid site, kills cells resistant to paclitaxel and epothilones, and may not require its epoxide moiety for activity. Biochemistry. 2002; 41:9109–9115. [PubMed: 12119025]
6. Gaitanos TN, Buey RM, Díaz JF, Northcote PT, Teesdale-Spittle P, Andreu JM, Miller JH. Peloruside A does not bind to the taxoid site on β-tubulin and retains its activity in multidrug-resistant cell lines. Cancer Res. 2004; 64:5063–5067. [PubMed: 15289305]
7. Bollag DM, McQueney PA, Zhu J, Hensens O, Koupal L, Liesch J, Goetz M, Lazarides E, Woods CM. Epothilones, a new class of microtubule-stabilizing agents with a taxol-like mechanism of action. Cancer Res. 1995; 55:2325–2333. [PubMed: 7757983]
8. Kowalski RJ, Giannakakou P, Gunasekera SP, Longley RE, Day BW, Hamel E. The microtubule-stabilizing agent discodermolide competitively inhibits the binding of paclitaxel (Taxol) to tubulin polymers, enhances tubulin nucleation reactions more potently than paclitaxel, and inhibits the growth of paclitaxel-resistant cells. Mol Pharmacol. 1997; 52:613–622. [PubMed: 9380024]
9. Edler MC, Buey RM, Gussio R, Marcus AI, Vanderwal CD, Sorensen EJ, Diaz JF, Giannakakou P, Hamel E. Cyclostreptin (FR182877), an Antitumor Tubulin-Polymerizing Agent Deficient in Enhancing Tubulin Assembly Despite Its High Affinity for the Taxoid Site. Biochemistry. 2005; 44:11525–11538. [PubMed: 16114889]
10. Buey RM, Barasoain I, Jackson E, Meyer A, Giannakakou P, Paterson I, Mooberry S, Andreu JM, Díaz JF. Microtubule interactions with chemically diverse stabilizing agents: Thermodynamics of binding to the paclitaxel site predicts cytotoxicity. Chem Biol. 2005; 12:1269–1279. [PubMed: 16356844]
11. Díaz JF, Barasoain I, Andreu JM. Fast kinetics of Taxol binding to microtubules. Effects of solution variables and microtubule-associated proteins. J Biol Chem. 2003; 278:8407–8419. [PubMed: 12496245]
12. Díaz JF, Barasoain I, Souto AA, Amat-Guerri F, Andreu JM. Macromolecular accessibility of fluorescent taxoids bound at a paclitaxel binding site in the microtubule surface. J Biol Chem. 2005; 280:3928–3937. [PubMed: 15550392]
13. Nogales E, Whittaker M, Milligan RA, Downing KH. High-resolution model of the microtubule. Cell. 1999; 96:79–88. [PubMed: 9989499]
14. Barasoain I, Garcia-Carril AM, Matesanz R, Maccari G, Trigili M, Mori M, Shi JZ, Fang WS, Andreu JM, Botta M, Díaz JF. Probing the pore drug binding site of microtubules with fluorescent taxanes: Evidence of two binding poses. Chem Biol. 2010; 17:243–253. [PubMed: 20338516]
15. Canales A, Salarichs JR, Trigili C, Nieto L, Coderch C, Andreu JM, Paterson I, Jiménez-Barbero J, Díaz JF. Insights into the interaction of discodermolide and docetaxel with dimeric tubulin. Mapping the binding sites of microtubule-stabilizing agents using an integrated NMR and computational approach. ACS Chemical Biology. 2011; 6:789–799. [PubMed: 21539341]
16. Bai R, Pei XF, Boye O, Getahun Z, Grover S, Bekisz J, Nguyen NY, Brossi A, Hamel E. Identification of cysteine 354 of β-tubulin as part of the binding site for the A ring of colchicine. J Biol Chem. 1996; 271:12639–12645. [PubMed: 8647876]
17. Calvo E, Camafeita E, Díaz JF, Lopez JA. Mass Spectrometry for Studying the Interaction between Small Molecules and Proteins. Current Proteomics. 2008; 5:20–34.
18. Sato B, Muramatsu H, Miyauchi M, Hori Y, Takase S, Hino M, Hashimoto S, Terano H. A new antimitotic substance, FR182877. I. Taxonomy, fermentation, isolation, physico-chemical properties and biological activities. J Antibiot (Tokyo). 2000; 53:123–130. [PubMed: 10805571]
19. Sato B, Nakajima H, Hori Y, Hino M, Hashimoto S, Terano H. A new antimitotic substance, FR182877. II. The mechanism of action. J Antibiot (Tokyo). 2000; 53:204–206. [PubMed: 10805584]

20. Buey RM, Calvo E, Barasoain I, Pineda O, Edler MC, Matesanz R, Cerezo G, Vanderwal CD, Day BW, Sorensen EJ, Lopez JA, Andreu JM, Hamel E, Díaz JF. Cyclostreptin binds covalently to microtubule pores and lumenal taxoid binding sites. Nature Chem Biol. 2007; 3:117–125. [PubMed: 17206139]
21. Shabbits JA, Krishna R, Mayer LD. Molecular and pharmacological strategies to overcome multidrug resistance. Expert Rev Anticancer Ther. 2001; 1:585–594. [PubMed: 12113091]
22. Tan B, Piwnica-Worms D, Ratner L. Multidrug resistance transporters and modulation. Curr Opin Oncol. 2000; 12:450–458. [PubMed: 10975553]
23. Bai R, Vanderwal CD, Diaz JF, Hamel E. Interaction of a cyclostreptin analogue with the microtubule taxoid site: the covalent reaction rapidly follows binding. J Nat Prod. 2008; 71:370–374. [PubMed: 18298077]
24. Andreu, JM. Tubulin Purification. In: Zhou, J., editor. Methods in Molecular Medicine. Totowa, NJ: Humana Press Inc.; 2007. p. 17-28.
25. Vanderwal CD, Vosburg DA, Weiler S, Sorensen EJ. An enantioselective synthesis of FR182877 provides a chemical rationalization of its structure and affords multigram quantities of its direct precursor. J Am Chem Soc. 2003; 125:5393–5407. [PubMed: 12720453]
26. Díaz, JF.; Buey, RM. Characterizing Ligand-Microtubule Binding by Competition Methods. In: Zhou, J., editor. Methods in Molecular Medicine. Totowa, NJ: Humana Press Inc.; 2007. p. 245-260.
27. Yang C, Barasoain I, Li X, Matesanz R, Liu R, Sharom FJ, Díaz JF, Fang W. Overcoming Tumor Drug Resistence Mediated by P-glycoprotein Overexpression with high affinity taxanes: A SAR study of C-2 Modified 7-Acyl-10-Deacetil Cephalomannines. Chem Med Chem. 2007; 2:691–701. [PubMed: 17385753]
28. Corton M, Botella-Carretero JI, Lopez JA, Camafeita E, Millan JLS, Escobar-Morreale HF, Peral B. Proteomic analysis of human omental adipose tissue in the polycystic ovary syndrome using two-dimensional difference gel electrophoresis and mass spectrometry. Human Reproduction. 2008; 23:651–661. [PubMed: 18156650]
29. Perez-Perez R, Ortega-Delgado FJ, Garcia-Santos E, Lopez JA, Camafeita E, Ricart W, Fernandez-Real JM, Peral B. Differential proteomics of omental and subcutaneous adipose tissue reflects their unalike biochemical and metabolic properties. J Proteome Res. 2009; 8:1682–1693. [PubMed: 19714809]
30. Shevchenko A, Tomas H, Havlis J, Olsen JV, Mann M. In-gel digestion for mass spectrometric characterization of proteins and proteomes. Nat. Protoc. 2006; 1:2856–2860. [PubMed: 17406544]
31. Perkins DN, Pappin DJ, Creasy DM, Cottrell JS. Probability-based protein identification by searching sequence databases using mass spectrometry data. Electrophoresis. 1999; 20:3551–3567. [PubMed: 10612281]
32. Pineda O, Farras J, Maccari L, Manetti F, Botta M, Vilarrasa J. Computational comparison of microtubule-stabilising agents laulimalide and peloruside with taxol and colchicine. Bioorg Med Chem Lett. 2004; 14:4825–4829. [PubMed: 15341932]
33. Spartan '08. Irvine, CA: Wavefunction, Inc.; 2008.
34. Shao Y, Molnar LF, Jung Y, Kussmann J, Ochsenfeld C, Brown ST, Gilbert ATB, Slipchenko LV, Levchenko SV, O'Neill DP, DiStasio RA, Lochan RC, Wang T, Beran GJO, Besley NA, Herbert JM, Lin CY, Van Voorhis T, Chien SH, Sodt A, Steele RP, Rassolov VA, Maslen PE, Korambath PP, Adamson RD, Austin B, Baker J, Byrd EFC, Dachsel H, Doerksen RJ, Dreuw A, Dunietz BD, Dutoi AD, Furlani TR, Gwaltney SR, Heyden A, Hirata S, Hsu CP, Kedziora G, Khalliulin RZ, Klunzinger P, Lee AM, Lee MS, Liang W, Lotan I, Nair N, Peters B, Proynov EI, Pieniazek PA, Rhee YM, Ritchie J, Rosta E, Sherrill CD, Simmonett AC, Subotnik JE, Woodcock HL, Zhang W, Bell AT, Chakraborty AK, Chipman DM, Keil FJ, Warshel A, Hehre WJ, Schaefer HF, Kong J, Krylov AI, Gill PMW, Head-Gordon M. Advances in methods and algorithms in a modern quantum chemistry program package. Phys. Chem. Chem. Phys. 2006; 8:3172–3191. [PubMed: 16902710]
35. Matesanz R, Barasoain I, Yang C, Wang L, Li X, De Ines C, Coderch C, Gago F, Jiménez-Barbero J, Andreu JM, Fang W, Díaz JF. Optimization of taxane binding to microtubules. Binding affinity decomposition and incremental construction of a high-affinity analogue of paclitaxel. Chem Biol. 2008; 15:573–585. [PubMed: 18559268]

36. Calvo E, Camafeita E, Fernández-Gutiérrez B, López JA. Applying selected reaction monitoring to targeted proteomics. Expert Review of Proteomics. 2011; 8:165–173. [PubMed: 21501010]
37. de Hoffmann E. Tandem mass spectrometry: A primer. Journal of Mass Spectrometry. 1996; 31:129–137.
38. Lowe J, Li H, Downing KH, Nogales E. Refined structure of α/β-tubulin at 3.5 A resolution. J Mol Biol. 2001; 313:1045–1057. [PubMed: 11700061]
39. Gigant B, Curmi PA, Martin-Barbey C, Charbaut E, Lachkar S, Lebeau L, Siavoshian S, Sobel A, Knossow M. The 4 Å X-ray structure of a tubulin:stathmin-like domain complex. Cell. 2000; 102:809–816. [PubMed: 11030624]
40. Ravelli RB, Gigant B, Curmi PA, Jourdain I, Lachkar S, Sobel A, Knossow M. Insight into tubulin regulation from a complex with colchicine and a stathmin-like domain. Nature. 2004; 428:198–202. [PubMed: 15014504]
41. Nogales E, Wolf SG, Downing KH. Structure of the α/β-tubulin dimer by electron crystallography. Nature. 1998; 391:199–203. [PubMed: 9428769]
42. Little M, Luduena RF. Structural differences between brain β1-tubulin and β2-tubulin implications for microtubule assembly and colchicine binding. EMBO J. 1985; 4:51–56. [PubMed: 4018027]
43. Medina JC, Roche D, Shan B, Learned RM, Frankmoelle WP, Clark DL, Rosen T, Jaen JC. Novel halogenated sulfonamides inhibit the growth of multidrug resistant MCF-7/ADR cancer cells. Bioorg Med Chem Lett. 1999; 9:1843–1846. [PubMed: 10406652]
44. Shan B, Medina JC, Santha E, Frankmoelle WP, Chou TC, Learned RM, Narbut MR, Stott D, Wu PG, Jaen JC, Rosen T, Timmermans P, Beckmann H. Selective, covalent modification of beta-tubulin residue Cys-239 by T138067, an antitumor agent with in vivo efficacy against multidrug-resistant tumors. Proc Natl Acad Sci U S A. 1999; 96:5686–5691. [PubMed: 10318945]
45. Hadvary P, Sidler W, Meister W, Vetter W, Wolfer H. The lipase inhibitor tetrahydrolipstatin binds covalently to the putative active site serine of pancreatic lipase. J Biol Chem. 1991; 266:2021–2027. [PubMed: 1899234]
46. Liu S, Widom J, Kemp CW, Crews CM, Clardy J. Structure of human methionine aminopeptidase-2 complexed with fumagillin. Science. 1998; 282:1324–1327. [PubMed: 9812898]
47. Chidester CG, Krueger WC, Mizsak SA, Duchamp DJ, Martin DG. The structure of CC-1065, a potent anti-tumor agent, and its binding to DNA. Journal of the American Chemical Society. 1981; 103:7629–7635.
48. Tomasz M, Chawla AK, Lipman R. Mechanism of monofunctional and bifunctional alkylation of DNA by Mitomycin-c. Biochemistry. 1988; 27:3182–3187. [PubMed: 3134045]
49. Evans DC, Watt AP, Nicoll-Griffith DA, Baillie TA. Drug-protein adducts: an industry perspective on minimizing the potential for drug bioactivation in drug discovery and development. Chem Res Toxicol. 2004; 17:3–16. [PubMed: 14727914]
50. Zhou SF, Chan E, Duan W, Huang M, Chen YZ. Drug bioactivation, covalent binding to target proteins and toxicity relevance. Drug Metab. Rev. 2005; 37:41–213. [PubMed: 15747500]
51. Reese M, Sanchez-Pedregal VM, Kubicek K, Meiler J, Blommers MJJ, Griesinger C, Carlomagno T. Structural basis of the activity of the microtubule-stabilizing agent epothilone A studied by NMR spectroscopy in solution. Angew Chem Int Ed Engl. 2007; 46:1864–1868. [PubMed: 17274084]
52. Sanchez-Pedregal VM, Kubicek K, Meiler J, Lyothier I, Paterson I, Carlomagno T. The tubulin-bound conformation of discodermolide derived by NMR studies in solution supports a common pharmacophore model for epothilone and discodermolide. Angew Chem Int Ed Engl. 2006; 45:7388–7394. [PubMed: 17036370]
53. Sanchez-Pedregal, VM.; Griesinger, C. The Tubulin Binding Mode of MT Stabilizing and Destabilizing. In: Carlomagno, T., editor. Tubulin-Binding Agents. Synthetic, Structural and Mecanistic Insights. Heidelberg: Springer; 2009. p. 151-208.
54. Bai RL, Covell DG, Pei XF, Ewell JB, Nguyen NY, Brossi A, Hamel E. Mapping the binding site of colchicinoids on β-tubulin 2-chloroacetyl-2-demethylthiocolchicine covalently reacts predominantly with cysteine 239 and secondarily with cysteine 354. J Biol Chem. 2000; 275:40443–40452. [PubMed: 11005811]

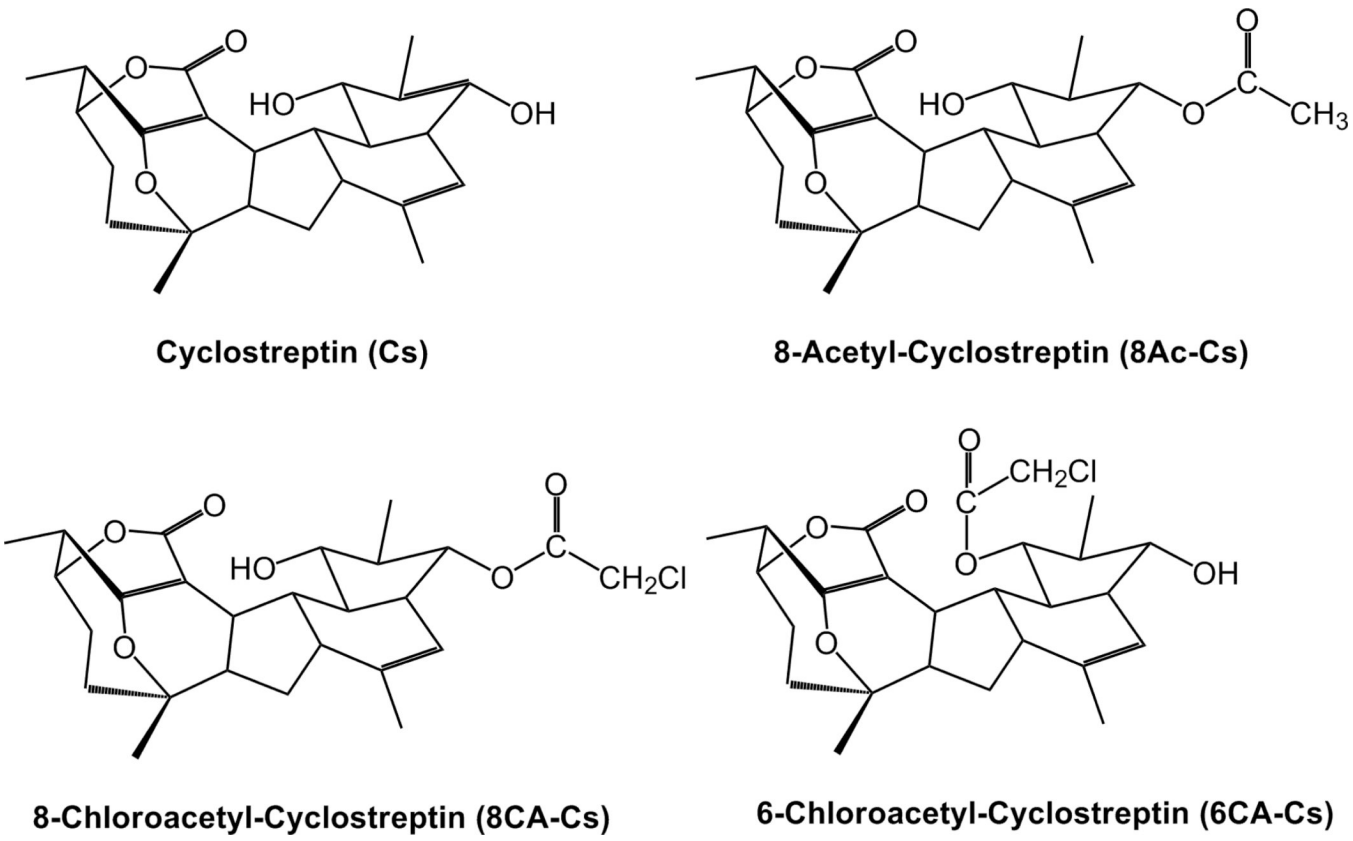

Figure 1.
Chemical structure of the Cs derivatives.

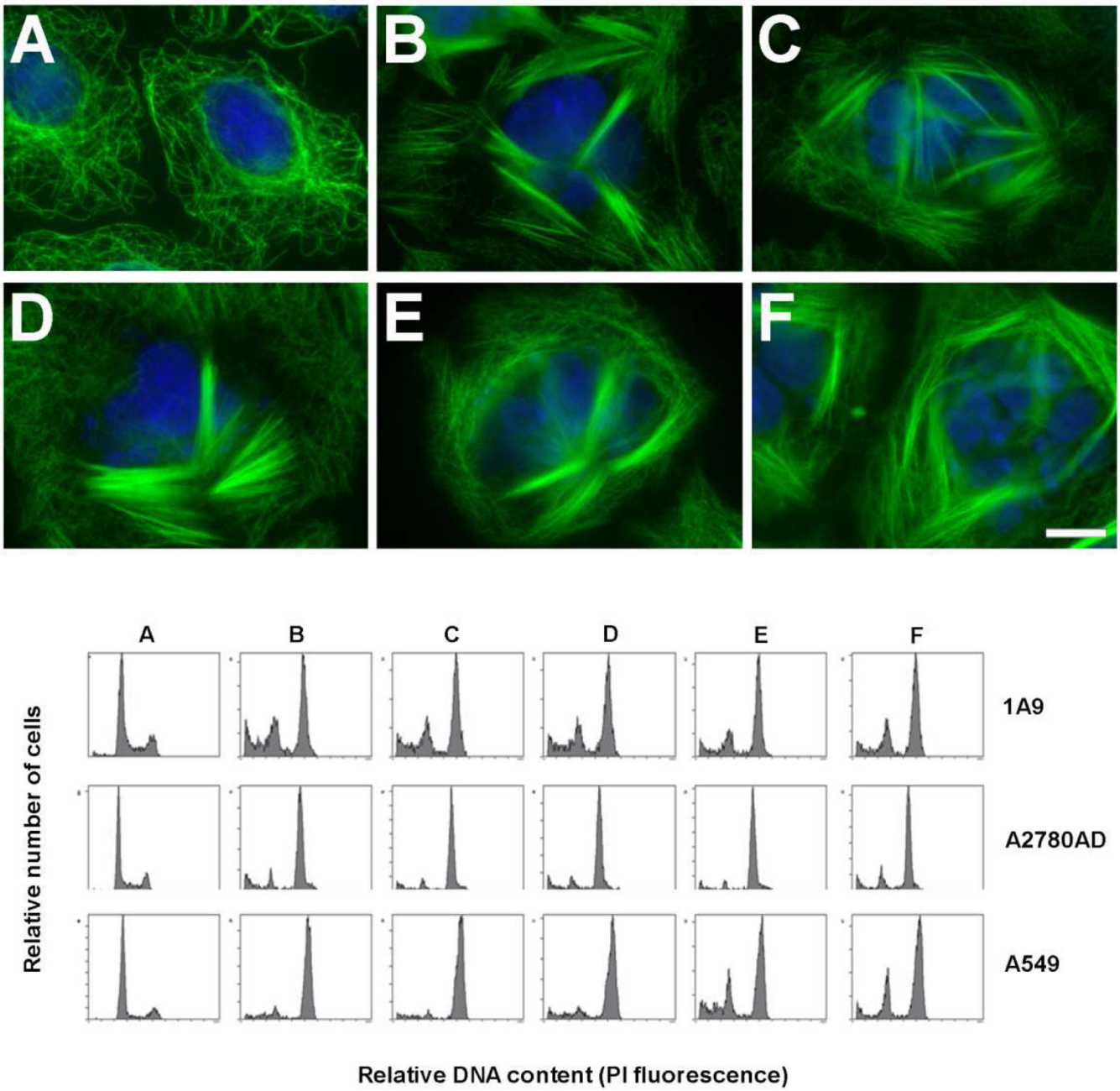

Figure 2.

Upper Panel. **Effect of Cs and derivatives on the cytoplasmic MTs of A549 cells**. Cells were incubated either with drug solvent (DMSO) (control cells) (A), 500 nM Cs (B), 2.5 μM 8Ac-Cs (C), 2.5 μM [^{14}C]8Ac-Cs (D), 5 μM 6CA-Cs (E) or 5 μM 8CA-Cs (F). MTs were immunostained with an α-tubulin monoclonal antibody, and DNA was stained with Hoechst 33342. Insets are mitotic cells from the same preparation. The scale bar represents 10 μm. Lower Panel. **Effect of Cs and derivatives on the cell cycle of 1A9, A2780AD and A549 cells.** Cells were incubated either with drug solvent (DMSO) (control cells) (A), 100 nM Cs (B), 400 nM 8Ac-Cs (C), 400 nM [^{14}C]8Ac-Cs (D), 200 nM 6CA-Cs (E) or 400 nM 8CA-Cs (F). The concentrations are those where maximal accumulation of cells in G2/M phase was observed. PI, propidium iodide.

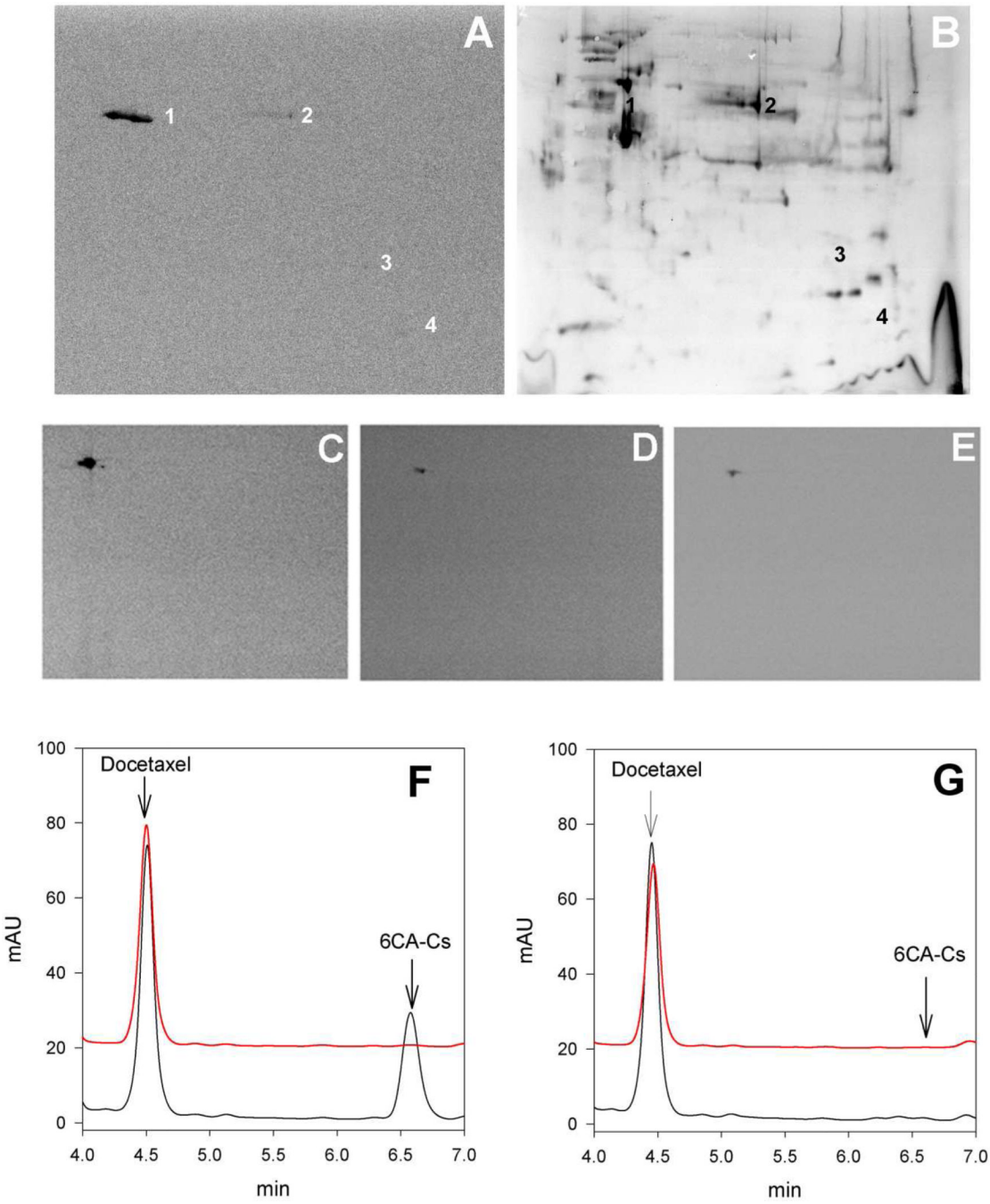

Figure 3.

Upper Panel **Identification of [^{14}C]8Ac-Cs protein cell targets.** Two dimensional gel electrophoresis of proteins extracted from A549 cells incubated with 2.5 μM [^{14}C]8Ac-Cs for 24 h. (A) Autoradiogram of the PDVF membrane after protein transfer. (B) The silver-stained 2D replica gel obtained with the protein extracts from treated cells and the spots corresponding to radiolabeled proteins are indicated (1 to 4). Protein identification was performed by in-gel trypsin digestion followed by database search with MALDI-TOF-MS data. Panels C,D,E.-[^{14}C]8Ac-Cs cell target is conserved in different cell lines. 1A9 cells incubated with 2.5 μM (C) or 300 nM [^{14}C]8Ac-Cs (D) and A549 cells incubated with 300

nM [^{14}C]8Ac-Cs (E). Lower Panel. **HPLC analysis of 6CA-Cs** extracted from pellets (red) and supernatants (black) after incubation without (F) and with (G) stabilized MTs.

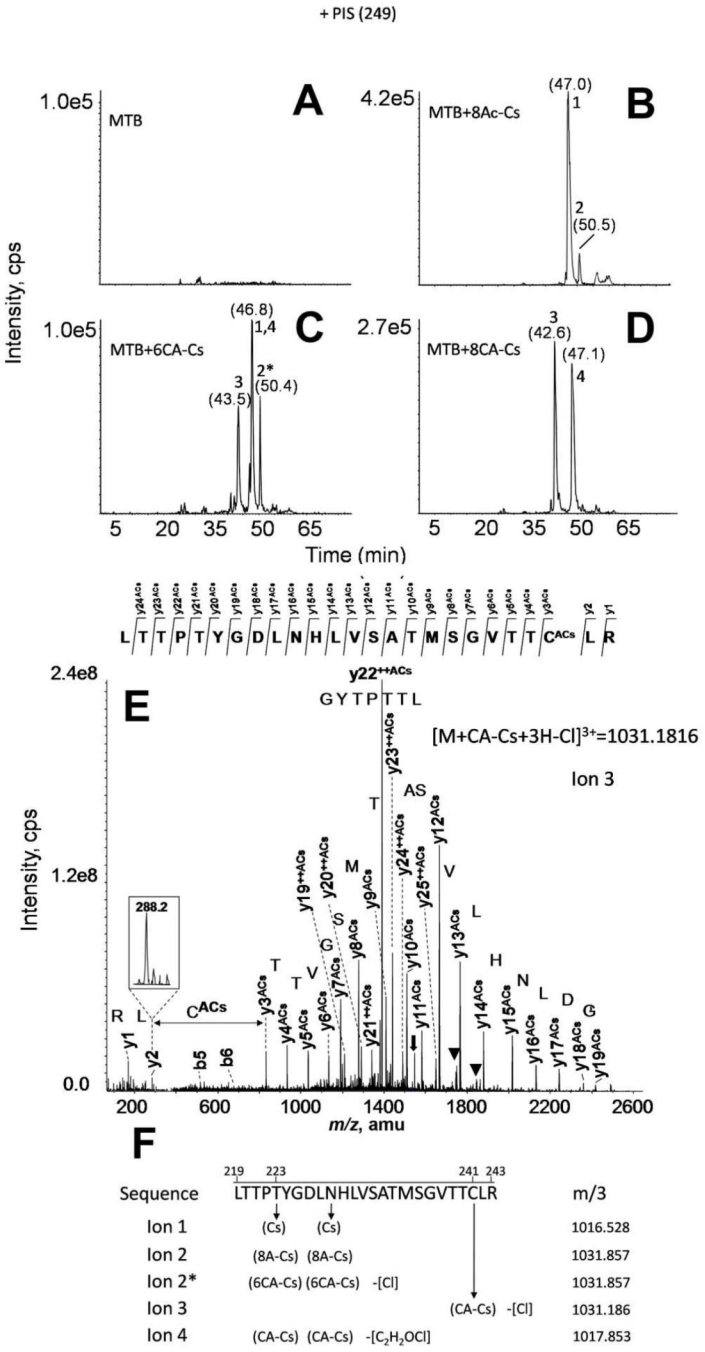

Figure 4.

MS analyses of Cs derivative binding to assembled MTs by PIS. Total ion chromatograms of the PIS experiments using the diagnostic ion at 249 *m/z* from control (A), or Cs derivative-treated, trypsin-digested MTs (MTB): 8Ac-Cs (B), 6CA-Cs (C), and 8CA-Cs (D). (E) Fragmentation spectrum from ion 3. Main fragmentation series (y-carboxy and b-amino) are indicated. Numbers above chromatographic peaks indicate the retention time (in brackets) and the type of detected ion. Water loss ions are indicated with black triangles. Doubly-charged fragment ions are labeled with ++, and a black arrow indicates the doubly-charged parent ion. (F) Hypothetical structure of Cs derivative adducts. A schematic structure for the hypothetical structure of ions 1 to 4 is presented. In brackets are marked the

linked group in each case attached to the corresponding residue through an arrow. The group loss in the different linkages is labeled in square brackets. m/3 indicate the exact mass observed for the triply-charged tubulin-derived adducts.

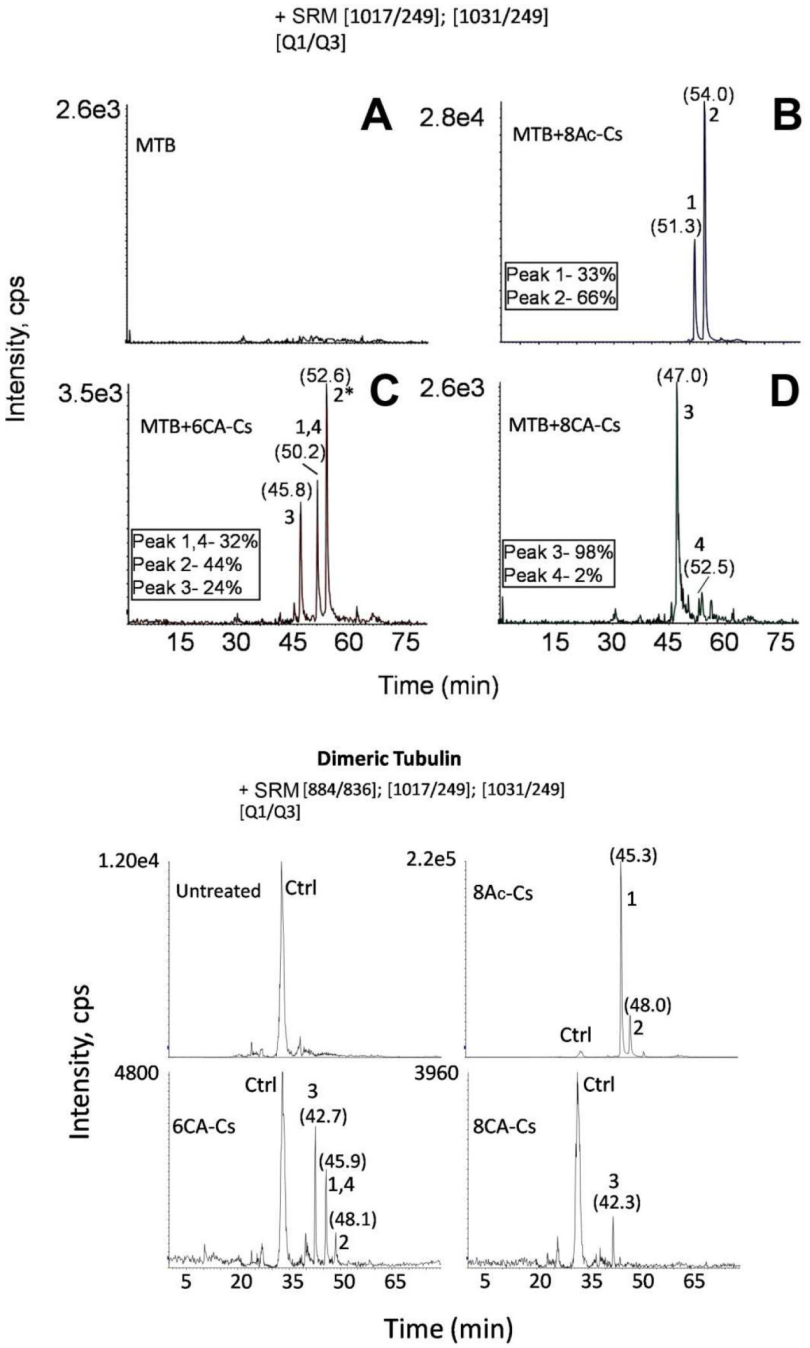

Figure 5.

Upper Panel **Estimation of adduct abundance by SRM.** Extracted ion chromatogram for the two ion pairs analyzed corresponding to Cs derivative linked adducts. The relative intensity percentage (numbered boxes) is indicated for ions detected in 8Ac-Cs-(B), 6CA-Cs- (C), and 8CA-Cs-treated MT samples (D). (A) Untreated MT sample. Numbers above chromatographic peaks indicate the retention time (in brackets) and the type of ion detected. Lower Panel **MS analyses of Cs derivative binding to dimeric tubulin by SRM.** Extracted ion chromatogram for SRM experiments of 3 ion pairs, including the ion pair corresponding to the tubulin-derived unmodified tryptic peptide (Q1 884 *m/z*, Q3 836 *m/z*,

labeled as Ctrl) in dimeric tubulin samples. Numbers above chromatographic peaks indicate the retention time (in brackets) and the type of detected ion.

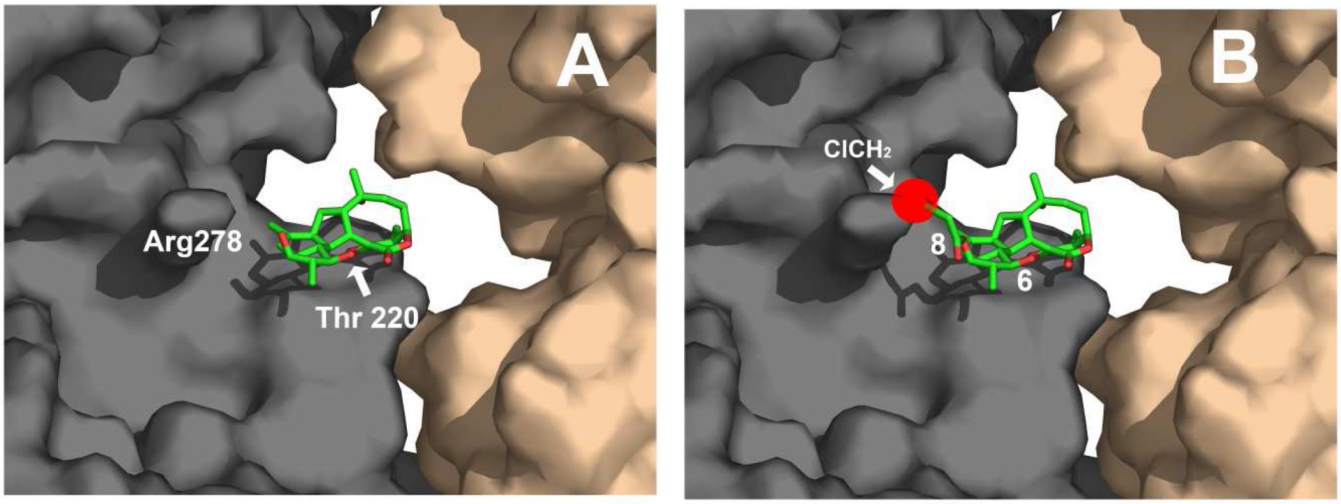

Figure 6.

Molecular models of: (A) Cs bound to Thr220 in the pore binding site of MTs as described in (20) and (B) 8CA-Cs placed in the same binding pose to show the steric hindrance that would result from the presence of the chloroacetyl moiety at position 8 (red sphere).

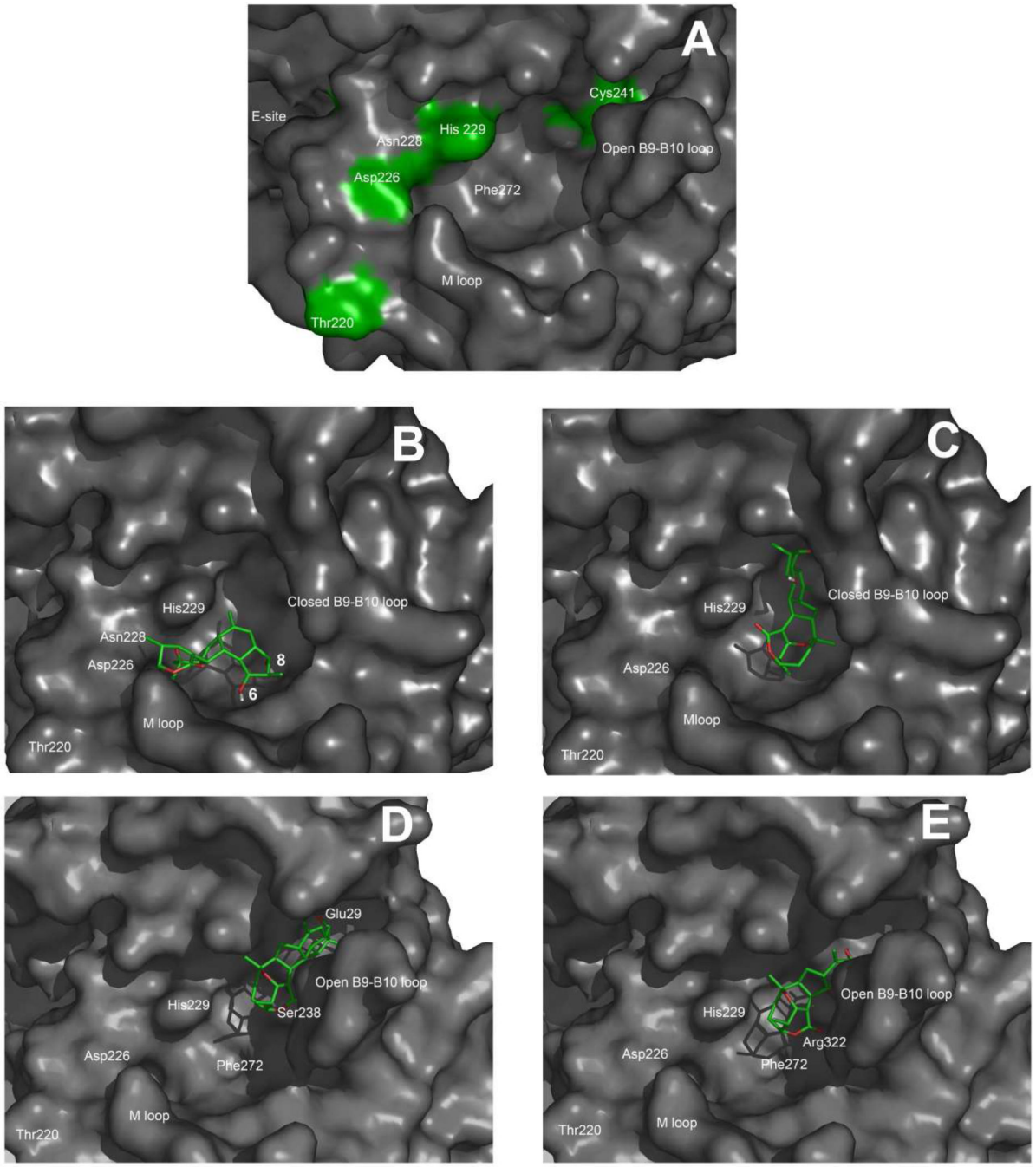

Figure 7.

Molecular models of: (A) The extended luminal pore site of PTX in MTs, (B) Cs docked into the luminal site (first pose), (C) Cs docked into the luminal site (second pose). (D) 6CA-Cs bound to Cys241 in the extended luminal site and (E) 8CA-Cs bound to Cys241 in the extended luminal site.

Table 1

Cytotoxicity of Cs and derivatives on the growth of two human ovarian carcinoma cell lines.[a]

Drug	1A9 (nM)[b]	A2780AD (nM)[b]	R/ S[c]
Cs	38 ± 4	46 ± 5	1.2
8Ac-Cs	152 ± 31	280 ± 23	1.7
[^{14}C]8Ac-Cs	100 ± 7	140 ± 12	1.4
6CA-Cs	84 ± 18	72 ± 24	0.8
8CA-Cs	192 ± 2	510 ± 40	2.6

[a] IC50 of the ligands determined in ovarian carcinoma cells 1A9 (a clone of A2780) and P-gp-over-expressing A2780AD.

[b] IC50 values (nM) are the mean ± standard error of at least three independent assays.

[c] The relative resistance of the A2780AD cell line obtained by dividing the IC50 of the resistant cell line by that of the parental 1A9 cell line.